



Attribution of the 3.45 eV GaN nanowires luminescence to inversion domain boundaries

Thomas Auzelle, Benedikt Haas, Martien den Hertog, Jean-Luc Rouvière,
Bruno Daudin, Bruno Gayral

► To cite this version:

Thomas Auzelle, Benedikt Haas, Martien den Hertog, Jean-Luc Rouvière, Bruno Daudin, et al.. Attribution of the 3.45 eV GaN nanowires luminescence to inversion domain boundaries. Applied Physics Letters, 2015, 107 (5), pp.051904. 10.1063/1.4927826 . hal-01586122

HAL Id: hal-01586122

<https://hal.science/hal-01586122>

Submitted on 26 May 2021

HAL is a multi-disciplinary open access archive for the deposit and dissemination of scientific research documents, whether they are published or not. The documents may come from teaching and research institutions in France or abroad, or from public or private research centers.

L'archive ouverte pluridisciplinaire **HAL**, est destinée au dépôt et à la diffusion de documents scientifiques de niveau recherche, publiés ou non, émanant des établissements d'enseignement et de recherche français ou étrangers, des laboratoires publics ou privés.

Attribution of the 3.45 eV GaN nanowires luminescence to inversion domain boundaries

Cite as: Appl. Phys. Lett. **107**, 051904 (2015); <https://doi.org/10.1063/1.4927826>

Submitted: 21 May 2015 . Accepted: 23 July 2015 . Published Online: 05 August 2015

 Thomas Auzelle, Benedikt Haas, Martien Den Hertog, Jean-Luc Rouvière, Bruno Daudin, and Bruno Gayral



View Online



Export Citation



CrossMark

ARTICLES YOU MAY BE INTERESTED IN

Luminescence properties of defects in GaN

Journal of Applied Physics **97**, 061301 (2005); <https://doi.org/10.1063/1.1868059>

The influence of AlN buffer over the polarity and the nucleation of self-organized GaN nanowires

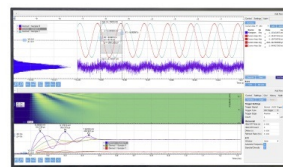
Journal of Applied Physics **117**, 245303 (2015); <https://doi.org/10.1063/1.4923024>

Polarity conversion of GaN nanowires grown by plasma-assisted molecular beam epitaxy

Applied Physics Letters **114**, 172101 (2019); <https://doi.org/10.1063/1.5094627>

Challenge us.

What are your needs for
periodic signal detection?



Zurich
Instruments



Attribution of the 3.45 eV GaN nanowires luminescence to inversion domain boundaries

Thomas Auzelle,^{1,a)} Benedikt Haas,² Martien Den Hertog,³ Jean-Luc Rouvière,² Bruno Daudin,¹ and Bruno Gayral¹

¹Université Grenoble Alpes, CEA-CNRS, NPSC, F-38054 Grenoble, France

²Université Grenoble Alpes, CEA-INAC/UJF-Grenoble1, SP2M, LEMMA, F-38054 Grenoble, France

³Université Grenoble Alpes, CNRS, Institut Néel, F-38042 Grenoble, France

(Received 21 May 2015; accepted 23 July 2015; published online 5 August 2015)

Using correlated experiments on single nanowires (NWs) by microphotoluminescence (μ -PL) and high resolution scanning transmission electron microscopy, we attribute the 3.45 eV luminescence of GaN NWs grown by plasma assisted molecular beam epitaxy (PA-MBE) to the presence of prismatic inversion domain boundaries (pIDBs). This attribution is further strengthened by a recent publication demonstrating the observation of pIDBs in PA-MBE grown GaN NWs. A statistical study of the presence of 3.45 eV lines in NWs PL spectra allows to estimate the ratio of single NWs nucleating with a pIDB to be 50% in the sample under scrutiny. © 2015 AIP Publishing LLC. [<http://dx.doi.org/10.1063/1.4927826>]

A remarkable difference between the photoluminescence (PL) spectra of bulk GaN or thin films and GaN nanowires (NWs) is the higher intensity of the sub-bandgap transition at 3.45 eV, observed in NWs at 10 K.¹ The surface over volume ratio being high in such system, the two major invoked reasons for this abnormally high intensity concerned subsurface excitonic recombinations. Corfdir *et al.*² have attributed the 3.45 eV band to two-electron-satellite (TES) excitonic recombinations on a near-surface donor and both Furtmayr *et al.*³ and Brandt *et al.*⁴ have tentatively assigned the band to excitonic recombinations on near-surface point defects. However, later magneto-luminescence experiments and a polarization-resolved study performed on the 3.45 eV band by Sam-Giao *et al.*⁵ convincingly refuted those two existing hypotheses.

In this report, based on a correlated PL and high resolution scanning transmission electron microscopy (HR-STEM) analysis on single NWs, we experimentally demonstrate that the 3.45 eV band is related to the presence of prismatic inversion domain boundaries (pIDBs) in GaN NWs.

This correlation is in accordance with the previous PL⁶ and cathodoluminescence (CL)⁷ measurements done on intentionally grown pIDB in GaN thin films. However, the case of NWs differs by a better spectral resolution of the lines assigned to the presence of a pIDB, noticeably because the pIDB is surrounded by high quality GaN. Additionally, the ability to disperse and isolate single NWs allows to probe a very small surface of pIDB (down to $0.03 \mu\text{m}^2$), which increases the chance of having a uniform environment, leading to a reduced spectral broadening.

At last, Robins *et al.*⁸ first suggested the origin of the 3.45 eV band in NWs to IDBs. At that time, this hypothesis has been discarded,^{2,3,5} as the polarity of self-organized NWs was still under debate and the existence of IDs ignored. Since it has been reported that a non-negligible fraction of GaN NWs grown on Si with an AlN buffer could host IDs,⁹ suggesting that pIDBs could be a common defect in NWs.

NWs were grown by plasma assisted molecular beam epitaxy (PA-MBE) on a 2-in. Si(111) substrate. Deoxidation of the silicon was done by dipping the wafer in a 10% HF solution for 10 s followed by a rinsing for a few minutes in deionized water. A last *in situ* annealing to 950 °C was done for a few minutes. The effective deoxidation of the wafer was checked by the observation of a clear 7×7 surface reconstruction at 820 °C. The growth temperature, set at 820 °C, was determined by the measurement of the corresponding Ga desorption time.¹⁰ A thin AlN buffer (2–3 nm thick) was grown directly onto the silicon. First, 2.4 monolayers (MLs) of Al were deposited on the bare silicon, followed by the nitridation. This alternate deposition of Al and N atoms was repeated four times. Then, GaN NWs were nucleated on the AlN buffer, and growth was performed in the conventional N-rich condition (Ga/N ratio of 0.3) for more than 10 h.¹¹ The result is a dense assembly of $2.3 \mu\text{m}$ long NWs with a density of $1.2 \times 10^{10} \text{ NW cm}^{-2}$. Long NWs were grown to ensure their easier localization by optical microscopy and to increase the amount of luminescent material once dispersed. Scanning electron microscopy (SEM) images of the NWs bottom (not shown here) revealed that a majority of NWs is the result of the coalescence of two or more single NWs, especially for extensive growth duration. Hence, we identified two types of NWs in the investigated sample: single NWs and coalesced NWs.

The as-grown NWs were dispersed onto a home-made 50 nm thick Si_3N_4 membrane, which allows combined STEM and μ -PL observations on the same NW.

For the dispersion, NWs were detached from their substrate and transferred into an ethanol solution using an ultrasonic bath. Next, droplets of the solution were deposited on the membrane, previously heated to 60 °C, which allows to obtain a uniform dispersion with an average density of $3 \times 10^{-2} \text{ object } \mu\text{m}^{-2}$.

The Si_3N_4 membrane was fabricated starting from a $300 \mu\text{m}$ thick Si (100) wafer with a layer of stoichiometric Si_3N_4 of 50 nm on each side. The fabrication procedure is described in Ref. 12. Optical deep ultraviolet lithography and

^{a)}Electronic mail: thomas.auzelle@cea.fr

electron beam metallization were used to pattern Ti-Au markers on the membranes to locate the same NW in different experiments.

μ -PL experiments were performed in a helium flow cryostat, using a continuous-wave frequency-doubled beam at 244 nm. The focused excitation spot size was about 1 μ m in diameter, using a 0.4 numerical aperture microscope objective. The luminescence signal from the sample was collected through the same optics and guided to a Jobin-Yvon Triaxe550 monochromator equipped with a 1200 grooves.mm⁻¹ grating and an ultraviolet-enhanced charge-coupled camera cooled down by liquid nitrogen. The sample surface was imaged on a CCD camera, allowing a precise localization of the NWs, relatively to the excitation spot and to the membrane markers. Fine tuning of the beam position on the NWs was done by optimizing the collected PL intensity. Prior to μ -PL, a mapping of NWs position on the grid was performed via a short SEM observation, working at low magnification and 10 kV.

NWs were observed by HR-STEM in a FEI Titan Ultimate working at 200 kV. pIDBs were imaged in the [11 $\bar{2}$ 0] zone axis, in high-angle annular dark field (HAADF) mode.

A PL spectrum taken at 10 K on the ensemble of as-grown NWs is shown in Figure 1(a). The band edge luminescence at 3.472 eV is attributed to the D_0X_A , and the tail at higher energy to the free exciton X_A . The luminescence band in the focus of this study is visible at 3.45 eV. It is composed of two lines centered at 3.450 and 3.457 eV with a respective line-width of 6.5 and 4.5 meV, which are larger than the 2.5 meV line-width of the D_0X_A .

After dispersion of the NWs on the Si₃N₄ membrane, μ -PL spectra were acquired on 73 objects. Later, SEM observations of the probed areas have shown that the objects could be classified in three types, exemplified in Figure 2: single NWs, coalesced NWs (from growth), and NW bunches that have aggregated during the dispersion. Considering coalesced NWs as the sum of individual single NWs, the average number of single NWs per probed object is three.

Three representative μ -PL spectra of dispersed objects are displayed in Figure 1(b). They are composed of several

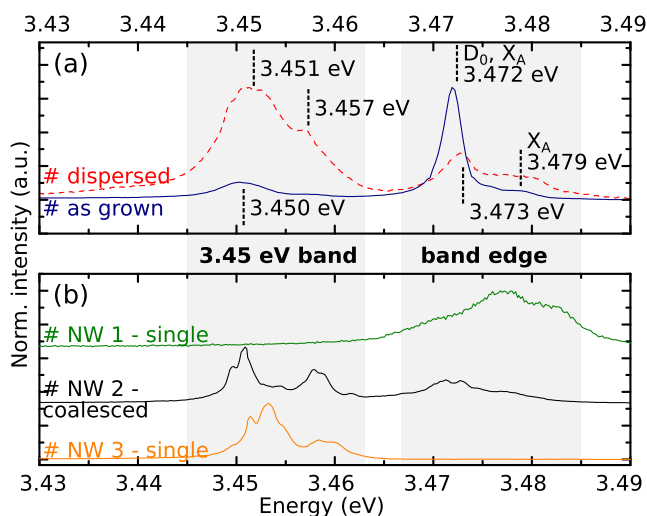


FIG. 1. (a) Normalized average PL spectra of $\sim 10^8$ as-grown NWs and about 73 dispersed NWs. (b) PL spectra of three different dispersed NWs. NWs were dispersed on an Si₃N₄ membrane. All acquisitions were done at 10 K.

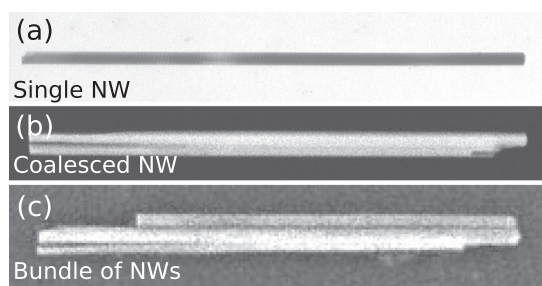


FIG. 2. (a) STEM image of a single NW. (b) and (c) SEM image of, respectively, a coalesced NW and a bundle of NWs.

sharp peaks with line-widths in the range of 1 meV. Peak position and relative intensity vary between the probed objects. Interaction with the substrate¹³ or variability between NWs^{2,4} can be invoked to explain such phenomena. Nevertheless, if averaged over the 73 probed objects, the PL spectra become similar to the one of as-grown NWs, as shown in Figure 1(a). Especially, no overlapping of the 3.45 eV band with the band edge is observed, meaning that both remain identifiable on dispersed NWs. Hence, from now on, for dispersed NWs, luminescence in the 3.445 – 3.463 eV range will be attributed to the 3.45 eV band and luminescence in the 3.467 – 3.485 eV range will be attributed to the band edge.

The average intensity of the 3.45 eV band is observed to increase relative to the band edge peak if probing dispersed NWs. This is attributed to the orthogonal polarization of the two considered radiation centers.⁵ The light collection axis being normal to the sample plane, the collection efficiency of a PL line is maximal when the dipole is parallel to the surface, i.e., when NWs are as-grown for the D_0X_A and when NWs are laying on the sample surface for the 3.45 eV lines.

In the spectra acquired on the single NWs, luminescence was observed in the band edge or in the 3.45 eV band but never in both at the same time. Despite a small statistic for single NWs (3 NWs), it suggests that the presence of a 3.45 eV line is quenching the band edge luminescence in single NWs. This conclusion can be further strengthened by looking at PL spectra acquired on more than one single NW. Indeed, if probing n single NWs at the same time, the probability to observe a luminescence only in the 3.45 eV band should follow a binomial law expressed as

$$P_{3.45 \text{ eV only}} = r^n. \quad (1)$$

r being the probability of having a 3.45 eV line in only one single NW. In a similar way, the probability to observe a luminescence only in the band edge should be

$$P_{\text{band edge only}} = (1 - r)^n. \quad (2)$$

At last, the probability to observe a luminescence in both the band edge and the 3.45 eV band is derived from the two other probabilities

$$P_{\text{both bands}} = 1 - [r^n + (1 - r)^n]. \quad (3)$$

Thanks to SEM observations, the number of single NWs in 59 probed objects has been estimated. In each pool of objects with the same amount of single NWs, the measurement frequency of PL spectra featuring only 3.45 eV lines or

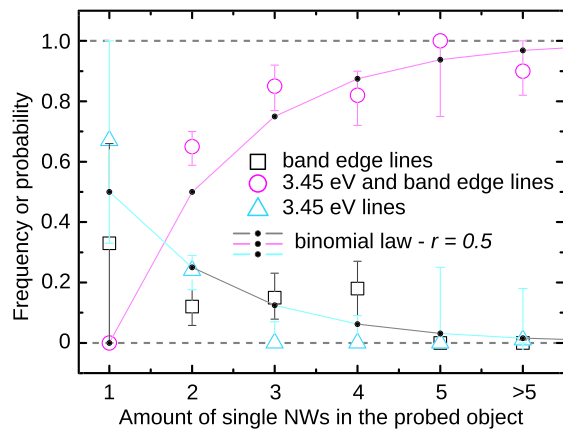


FIG. 3. For probed objects with the same amount of single NWs, the frequency of PL spectra belonging to a defined category: having PL lines in the 3.45 eV band and/or in the band edge is plotted. The error bars indicate the frequency shift if one PL spectra of the specified category would have been erroneously attributed (-1 spectra for the category) or forgotten ($+1$ spectra for the category). Binomial probability is plotted as well.

only band edge lines or both has been calculated and compared to the probabilities given by the binomial law (Figure 3). The most satisfactory fit of the frequencies is reached for $r = 0.5$. It would mean that in this sample, half of the single NWs have a luminescence at 3.45 eV. This value stands as a rough estimation as the main and non-negligible uncertainty in this method lie in determining the amount of single NWs in each object, especially when dealing with coalesced NWs.

Next to μ -PL observations, the same NWs were imaged by HR-STEM. IDs were identified either by looking at the intensity patterns of HR-STEMs images (Figures 4(b) and 4(c)) or more systematically by measuring the displacement of the (0002) planes (Figure 4(e)). As exemplified in the IDB image of Figure 4(c), bright spots over the ID are elongated along the c axis whereas they are not in the unipolar area. Image simulations have shown that these elongated features are characteristic of the superposition of Ga- and N-polar slabs along the electron beam, the elongated spots containing two partial Ga columns shifted by $c/8$. Hence, a measure of the shift between the mass-center of the spots allows to detect or not the presence of IDs.

The presence of Ga-polar IDs has been evidenced in a significant number of NWs (single or coalesced ones). The IDs are located in the core of the NWs and propagate from the bottom to the top, along the c axis, as sketched in Figure 4(f). NWs contain either one or no ID.

The systematic correlated observation of NW atomic structure and its PL reveals, as exemplified in Figure 4, that a luminescence in the 3.45 eV band always occurs if one of the probed NWs is hosting a pIDB. This correlation is also true for probed single NWs, meaning that coalescence in this sample did not generate extended defects¹⁴ acting as excitonic recombination centers. Hence, the 3.45 eV luminescence is attributed to an excitonic recombination on a pIDB.

The experimentally suggested quenching of the band edge luminescence due to the presence of a pIDB, in single NWs, is in accordance with the scheme of the IDB as a radiative localization center for excitons. Indeed, considering a diffusion length for excitons in NWs as low as 70 nm,¹⁵ the captured volume of the IDB would exceed by far the dimension of the full NW. It also suggests, from the statistical analysis on the measurement frequency of the 3.45 eV band, that approximately 50% of the single NWs are nucleating with a pIDB in the sample under scrutiny.

PL spectra do not exhibit the presence of deep states linked to the presence of the pIDB. It is in accordance with the theoretical model of the IDB* structure, which was calculated by *ab-initio* means as free of deep states.^{16,17} Additionally, it suggests that the pIDB does not getter point defects as theoretically predicted in ZnO.¹⁸

In summary, we performed a correlated PL study with STEM observations on the same NWs. A 3.45 eV luminescence was exclusively found in NWs hosting IDs, leading to the conclusion that the 3.45 eV band is the result of excitonic recombinations on a pIDB. This attribution could be further generalized to self-organized GaN NWs grown on Si by PAMBE, for which pIDBs were recently demonstrated to be a recurrent defect.⁹ Using a statistical approach, the ratio of single NWs nucleating with a pIDB is estimated to be 50% for the sample under scrutiny.

By using the presence of the 3.45 eV PL band as a marker of the presence of IDs, our results suggest that the GaN NWs

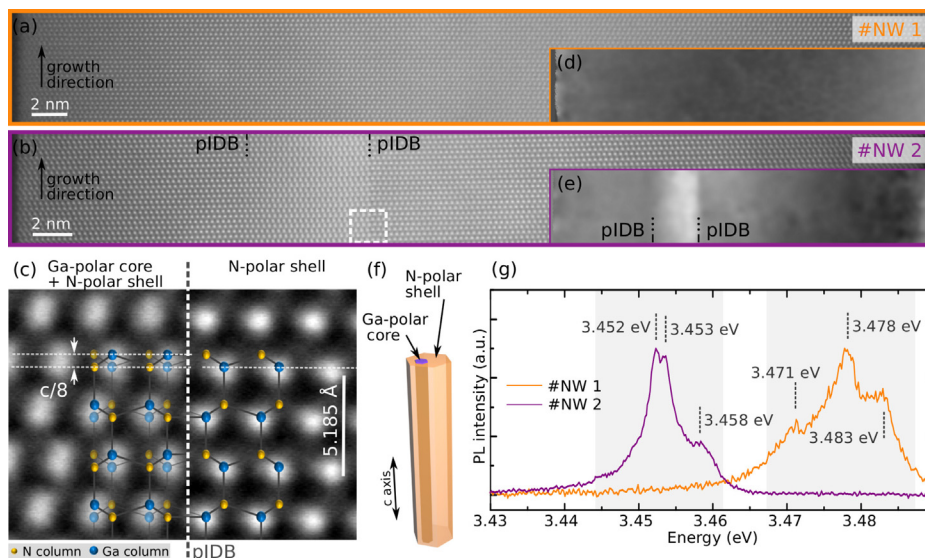


FIG. 4. (a) HR-HAADF-STEM image of #NW 1, which is free of IDs. (b) and (c) HR-HAADF-STEM images of #NW 2, which hosts a Ga-polar ID. (d) and (e) Images displaying the shift between (0002) planes in, respectively, #NW 1 and #NW 2. (f) Sketch of #NW 2 ID. (g) Comparative μ -PL spectra of #NW 1 and #NW 2, acquired at 10 K.

grown on Si(001) and on sapphire are hosting IDs as well, as both were reported to exhibit a 3.45 eV luminescence.^{1,2} More generally, we propose that the observation of the 3.45 eV line in a simple PL experiment is an efficient way of evidencing the presence of IDs in GaN nanostructures for which the donor bound exciton line is spectrally narrow enough.

This work was performed in the CEA/CNRS joint team “Nanophysics and semiconductors” of Institut Néel and INAC, and in the team “Materials Structure and Radiation” of Institut Néel. We have benefited from the access to the technological platform NanoCarac of CEA-Minatech and acknowledge help from the technical support team of Institut Néel: “Nanofab” (Bruno Fernandez). We acknowledge financial support from ANR programs JCJC (Project COSMOS, ANR-12-JS10-0002) and P2N (Project FIDEL, ANR-11-NANO-0029).

¹E. Calleja, M. A. Sánchez-García, F. J. Sánchez, F. Calle, F. B. Naranjo, E. Muñoz, U. Jahn, and K. Ploog, *Phys. Rev. B* **62**, 16826 (2000).

²P. Corfdir, P. Lefebvre, J. Risti, P. Valvin, E. Calleja, A. Trampert, J.-D. Ganire, and B. Deveaud-Plédran, *J. Appl. Phys.* **105**, 013113 (2009).

³F. Furtmayr, M. Vilemeyer, M. Stutzmann, A. Laufer, B. K. Meyer, and M. Eickhoff, *J. Appl. Phys.* **104**, 074309 (2008).

⁴O. Brandt, C. Pfüller, C. Chêze, L. Geelhaar, and H. Riechert, *Phys. Rev. B* **81**, 045302 (2010).

⁵D. Sam-Giao, R. Mata, G. Tourbot, J. Renard, A. Wyszomolek, B. Daudin, and B. Gayral, *J. Appl. Phys.* **113**, 043102 (2013).

⁶P. J. Schuck, M. D. Mason, R. D. Grober, O. Ambacher, A. P. Lima, C. Miskys, R. Dimitrov, and M. Stutzmann, *Appl. Phys. Lett.* **79**, 952 (2001).

⁷R. Kirste, R. Collazo, G. Callsen, M. R. Wagner, T. Kure, J. Sebastian Reparaz, S. Mita, J. Xie, A. Rice, J. Tweedie, Z. Sitar, and A. Hoffmann, *J. Appl. Phys.* **110**, 093503 (2011).

⁸L. H. Robins, K. A. Bertness, J. M. Barker, N. A. Sanford, and J. B. Schlager, *J. Appl. Phys.* **101**, 113506 (2007).

⁹T. Auzelle, B. Haas, A. Minj, C. Bougerol, J.-L. Rouvire, A. Cros, J. Colchero, and B. Daudin, *J. Appl. Phys.* **117**, 245303 (2015).

¹⁰O. Landré, R. Songmuang, J. Renard, E. Bellet-Amalric, H. Renevier, and B. Daudin, *Appl. Phys. Lett.* **93**, 183109 (2008).

¹¹M. Sanchez-Garcia, E. Calleja, E. Monroy, F. Sanchez, F. Calle, E. Muoz, and R. Beresford, *J. Cryst. Growth* **183**, 23 (1998).

¹²M. I. den Hertog, F. Gonzalez-Posada, R. Songmuang, J. L. Rouviere, T. Fournier, B. Fernandez, and E. Monroy, *Nano Lett.* **12**, 5691 (2012).

¹³R. Anufriev, N. Chauvin, H. Khmisi, K. Naji, M. Gendry, and C. Bru-Chévallier, *Appl. Phys. Lett.* **101**, 072101 (2012).

¹⁴K. Grossklau, A. Banerjee, S. Jahangir, P. Bhattacharya, and J. Millunchick, *J. Cryst. Growth* **371**, 142 (2013).

¹⁵G. Nogues, T. Auzelle, M. Den Hertog, B. Gayral, and B. Daudin, *Appl. Phys. Lett.* **104**, 102102 (2014).

¹⁶V. Fiorentini, *Appl. Phys. Lett.* **82**, 1182 (2003).

¹⁷J. E. Northrup, J. Neugebauer, and L. T. Romano, *Phys. Rev. Lett.* **77**, 103 (1996).

¹⁸Y. Yan and M. M. Al-Jassim, *Phys. Rev. B* **69**, 085204 (2004).